

# Isotopic fractionation in proteins as a measure of hydrogen bond length

Ross H. McKenzie\*

*School of Mathematics and Physics, University of Queensland, Brisbane 4072, Australia*

Bijyalaxmi Athokpam and Sai G. Ramesh

*Department of Inorganic and Physical Chemistry,  
Indian Institute of Science, Bangalore 560 012, India*

(Dated: December 7, 2021)

If a deuterated molecule containing strong intramolecular hydrogen bonds is placed in a hydrogenated solvent it may preferentially exchange deuterium for hydrogen. This preference is due to the difference between the vibrational zero-point energy for hydrogen and deuterium. It is found that the associated fractionation factor  $\Phi$  is correlated with the strength of the intramolecular hydrogen bonds. This correlation has been used to determine the length of the H-bonds (donor-acceptor separation) in a diverse range of enzymes and has been argued to support the existence of short low-barrier H-bonds. Starting with a potential energy surface based on a simple diabatic state model for H-bonds we calculate  $\Phi$  as a function of the proton donor-acceptor distance  $R$ . For numerical results, we use a parameterization of the model for symmetric O-H $\cdots$ O bonds [*Chem. Phys. Lett.* **535**, 196 (2012)]. We consider the relative contributions of the O-H stretch vibration, O-H bend vibrations (both in plane and out of plane), tunneling splitting effects at finite temperature, and the secondary geometric isotope effect. We compare our total  $\Phi$  as a function of  $R$  with NMR experimental results for enzymes, and in particular with an empirical parametrization  $\Phi(R)$ , used previously to determine bond lengths.

---

\* email: r.mckenzie@uq.edu.au; URL: condensedconcepts.blogspot.com

## I. INTRODUCTION

The issue of low-barrier hydrogen bonds in proteins and whether they play any functional role, particularly in enzyme catalysis, is controversial [1–10]. Identifying such short hydrogen bonds, characterised by a donor-acceptor distance of  $R \simeq 2.45\text{--}2.65 \text{ \AA}$ , is not completely straightforward [11]. In protein X-ray crystallography, the standard errors in inter-atomic distances are about 10 to 30 per cent of the resolution. Hence, for an X-ray structure with 2.0 Å resolution, the standard errors in the distances are  $\pm(0.2\text{--}0.6) \text{ \AA}$ . This uncertainty makes it difficult to distinguish between short strong bonds and the more common weak long bonds, with  $R > 2.8 \text{ \AA}$  [12]. NMR provides an alternative method of bond length determination via the  $^1\text{H}$  chemical shift. An independent NMR “ruler” involves isotopic fractionation, where one measures how much the relevant protons (H) exchange with deuterium (D) in a solvent.



Here Pr-H denotes a protein with a proton in the relevant hydrogen bond. The fractionation ratio can also be determined from UV spectroscopy [13].

The fractionation ratio is equilibrium constant of Eq. (1):

$$\Phi \equiv \frac{[\text{Pr} - \text{D}][\text{H}_{\text{solvent}}]}{[\text{Pr} - \text{H}][\text{D}_{\text{solvent}}]} \quad (2)$$

Translated into partition functions,  $\Phi$  is essentially determined by the relative zero-point energy (ZPE) of a D relative to an H in the protein. As described by Kreevoy and Liang [13], the ratio is given by

$$k_B T \ln \Phi = Z_{\text{H-Pr}} - Z_{\text{D-Pr}} + Z_{\text{D,solvent}} - Z_{\text{H,solvent}} \quad (3)$$

where  $T$  is the temperature and  $Z_{\text{H-Pr}}$  denotes the zero-point energy of a proton participating in the relevant hydrogen bond in the protein. Throughout this paper we set  $T = 300 \text{ K}$ .

Fractionation is a purely quantum effect. If the nuclear dynamics were classical, the fractionation ratio would be one. It would also be one if there were no changes in the vibrational frequencies — more correctly, zero-point energies — of both H and D when they moved from the solvent to the protein. However, the vibrational potentials *are* different in the two environments. The donor-acceptor distance,  $R$ , is typically shorter in the protein, indicating a stronger H-bond and a softer X-H stretch potential (X is the H-bond donor). Consequently, the difference between H and D zero-point energies gets larger [14], and  $\Phi$  gets smaller with decreasing  $R$ . However,

for very short bonds, typically when the donor and acceptor share the H or D atoms, the stretch frequencies begin to harden and  $\Phi$  starts to increase.  $\Phi$  then has a non-monotonic dependence on  $R$  [15].

Mildvan and collaborators [11, 16] considered a particular parametrisation of the H-bond potential to connect the observed fractionation ratio with donor-acceptor bond lengths in a range of proteins. They generally find reasonable agreement between determinations of the length from the fractionation factor and that from the NMR chemical shift. In particular, the uncertainty is less than that deduced from X-rays.

In this paper, we systematically investigate how the fractionation factor  $\Phi$  varies with the donor-acceptor distance  $R$ . Specifically, we consider the relative importance of different contributions to  $\Phi$ . We find that the competing quantum effects associated with the X-H stretch and bend modes are the most significant. Non-degeneracy of the two bend modes and tunnel splitting of the stretch mode have small but noticeable effects. The only important effect of the secondary geometric isotope effect is that it enhances the contribution from the tunnel splitting, mostly for  $R \sim 2.4\text{--}2.6$  Å. For most values of  $R$ , the value of  $\Phi$  we calculate differs from the empirical relation due to Mildvan et al. [16] that has been used to determine bond lengths in enzymes.

## II. METHOD

We calculate the H/D zero-point energies, and hence  $\Phi$ , with the electronic ground state potential of a two-diabatic state model [17]. For X and Y as donor and acceptor, the two diabatic states of the model are X-H $\cdots$ Y and X $\cdots$ H-Y, which are modelled as Morse oscillators. The coupling between the diabatals is a function of  $R$ , the X-Y distance, as well as the H-X-Y and H-Y-X angles; it decreases exponentially with increasing  $R$  and gets weaker with larger angular excursions of the H atom. Previously, we showed that this model can give a quantitative description of the correlations observed [18] for a diverse range of chemical compounds between  $R$  and X-H bond lengths, vibrational frequencies, and isotope effects [14].

We now briefly discuss the domain of applicability of this simple model to hydrogen bonds in proteins, which are certainly complex and diverse chemical systems. First, our focus is on a small (but potentially important) sub-class of hydrogen bonds: short strong bonds. Second, we consider the simplest possible model that might capture the essential features of these bonds, independent of the finer structural details of a specific protein. The goal is to obtain physical insight

into the different quantum effects that contribute to the fractionation factor, as well as their (non-monotonic) trends with donor-acceptor distance. H-bonds in proteins vary from weak to strong, and can further be modified by coupling to other neighbouring H-bonds [19]. Also important are the proximity to and accessibility to the solvent, and anisotropic electric fields arising from neighbouring charged amino acid residues. An example of the latter occurs in the Photoactive Yellow Protein (PYP) where the existence of a possible low barrier H-bond may be dependent on deprotonation of the neighbouring Arg52 residue [7, 20]. A key feature of the two-diabatic state model used here is that it takes the donor-acceptor bond distance and the  $\text{pK}_a$  difference as the key bond descriptors. These are input from available experimental information. These two parameters will certainly be modified by chemical substituents [21], solvent, and perturbations from the local electric field as indicated above. Description of multiple H-bonds requires generalisation of the model considered here to include more than two diabatic states [22].

The parametrization used in References 14 and 17 was for O-H $\cdots$ O symmetric hydrogen bonds, i.e. the donor and acceptor have the same proton affinity ( $\text{pK}_a$ ). In the present work, we retain this parametrization. This is an approximation for comparisons with H-bonds in proteins, which are generally asymmetric (donor and acceptor with different  $\text{pK}_a$ ). Many H-bonds in proteins are actually N-H $\cdots$ O bonds. However, as the H-bonds become stronger ( $R \lesssim 2.5 \text{ \AA}$ ) the equal proton affinity approximation becomes more reliable. At such distances, the donor and acceptor effectively share the H atom. In the diabatic state model, the off-diagonal coupling element becomes large enough to strongly suppress or eliminate the barrier for the H atom transfer. Kreevoy and Liang [13], Bao et al.[23], and Oltrogge and Boxer[21] considered how asymmetry in the one-dimensional proton transfer potential modifies the fractionation factor. Non-degeneracy smaller than  $800 \text{ cm}^{-1}$  (or equivalently, a  $\text{pK}_a$  difference of about 2) has only a small effect on the proton transfer potential and the fractionation factor when  $R < 2.5 \text{ \AA}$ .

The total vibrational zero-point energy for Pr-H/D is

$$Z(R) \equiv Z_{\parallel}(R) + Z_{\perp,o}(R) + Z_{\perp,i}(R). \quad (4)$$

The three terms are the zero-point energy associated with X-H vibrations parallel to the hydrogen bond (stretch), out-of-plane bend ( $o$ ), and in-plane bend ( $i$ ) of X-H $\cdots$ Y, respectively. (The plane typically refers to that of X-H.) The simple summation in the above equation points to our assumption that these modes are uncoupled.

The O-H/D stretch zero-point energy is calculated numerically by using the sinc-function Dis-

crete Variable Representation (DVR) [24] to solve the one-dimensional Schrodinger equation as a function of  $R$ . This gives an essentially exact treatment for the significant anharmonic and tunnelling effects that occur for low-barrier bonds [14].

We treat zero-point energies of bend modes as half their classical harmonic frequencies as a function of  $R$ . To break the degeneracy of the two modes, we use the result from the model itself that hardening of the two bend motions is similar:

$$\Omega_{\perp,o/i}(R)^2 = \omega_{\perp,o/i}^2 + 2f(R) \quad (5)$$

where  $\omega_{\perp,o/i}$  is the frequency in the absence of an H-bond and the function  $f(R)$  is given in Eqn. (6) of Ref. 17. At least in the  $R$  range of interest,  $f(R)$  is a positive function that monotonically decreases with increasing  $R$  (compare Figure 1). In general  $\omega_{\perp,i} > \omega_{\perp,o}$  and so  $\Omega_{\perp,i} > \Omega_{\perp,o}$ . Here we take  $\omega_{\perp,o} = 650 \text{ cm}^{-1}$  and  $\omega_{\perp,i} = 650$  or  $1600 \text{ cm}^{-1}$ . The  $\omega$  parameters for the deuterium isotope are taken to be  $\sqrt{2}$  smaller than for the H isotope.

Eq. (3) for  $\Phi$  assumes that only the ground state energies of the species is relevant (at the temperature of interest). For a symmetric proton transfer potential, one expects a first excited state due to tunnel splitting that would be close in energy to the ground state. In our model, this appears along the X-H stretch coordinate. Hence the first excited state for the H/D motion makes a further multiplicative contribution of the form

$$\Phi_{\text{tun}} = \frac{1 + \exp(-\delta E_D/k_B T)}{1 + \exp(-\delta E_H/k_B T)} \quad (6)$$

to the fractionation factor, where  $\delta E_{H/D} \equiv E_{0-} - E_{0+}$  is the tunnel splitting.

Another contribution to  $\Phi$  comes from the secondary geometric isotope effect (SGIE) where the X-Y distance changes upon deuteration. This is a subtle effect with a non-monotonic dependence on  $R$  [14, 25, 26]. As shown in Ref. 14 and references therein, it arises because the rates of change with  $R$  of the zero-point energy for H and D are different (compare Figure 1). The net effect is that true minima of the total system energy with respect to  $R$  for both H and D ( $R_H$  and  $R_D$ ) are shifted relative to the classical minimum ( $R_o$ ). The difference between the minima is largely under  $0.04 \text{ \AA}$  with  $R_D > R_H$ , but the resulting effects on frequencies are substantial. There are two consequences of SGIE for the fractionation ratio. First, the zero point energy for the H and D should be calculated at their respective minima. Second, an elastic energy associated with the stretching of the donor-acceptor distance, of the form  $\frac{1}{2}K(R_{H/D} - R_o)^2$ , must be included. Here,  $K$  is the elastic constant that is parametrised empirically in Ref. 14. We have included both consequences of the SGIE in our calculation.

The above details describe the calculation of the  $[\text{Pr-D}]/[\text{Pr-H}]$  part of  $\Phi$ , in Eq. (2), as a function of  $R$ . The corresponding ratio for the solvent is taken to be the calculated model value at  $R = 2.8$  Å, approximately the relevant length in water. Later we discuss how our results are not particularly sensitive to this exact choice of a reference distance.

### III. RESULTS AND DISCUSSION

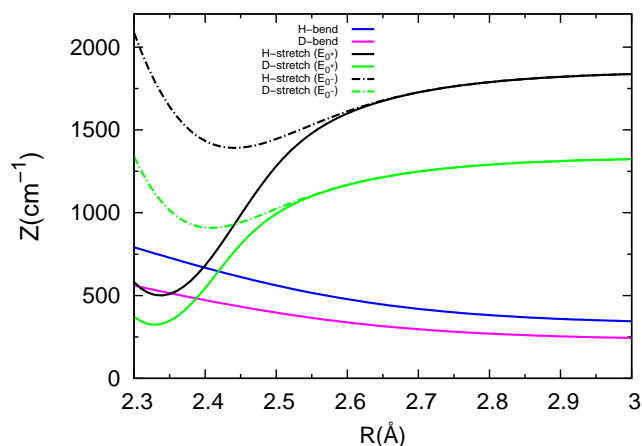


Figure 1. Competing quantum effects. The zero-point energies of the out-of-plane bend mode and of the two lowest stretch quantum states (due to tunnel splitting,  $E_{0\pm}$ ) are shown for both H and D isotopes as a function of the donor-acceptor distance  $R$ . The black curves [H-stretch ( $E_{0\pm}$ )] correspond to the stretch mode of the H isotope, while green curves [D-stretch ( $E_{0\pm}$ )] are those of the D isotope (solid: +, dot-dashed: -). Blue (H-bend) and magenta (D-bend) curves are out of plane bend zero-point energies for the H and D isotopes, respectively. With increasing  $R$ , the stretch zero-point energies increase and those of the bend decrease. Note how for  $R < 2.55$  Å (2.45 Å), the tunnel splitting of the stretch mode for the H (D) isotope becomes observable.

#### A. Role of competing quantum effects

Figure 1 shows the computed trends of the stretch and bend zero-point energies from the model for both H and D isotopes. The solid black (H) and green (D) curves show the O-H/D stretch zero-point energies. The limiting energies at large  $R$  are those of O-H and O-D bonds, about 1800 and 1300  $\text{cm}^{-1}$ , respectively. Of relevance to the fractionation factor  $\Phi$  is the *difference* between

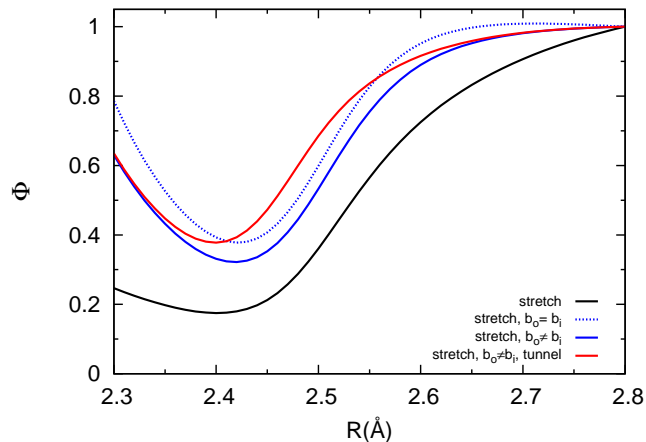


Figure 2. Effect of the bend modes and tunnel splitting on the fractionation ratio. The black curve (stretch) includes solely the effects of the X-H stretch vibrational mode. The blue curves include the effect of the in-plane ( $b_i$ ) and out-of-plane ( $b_o$ ) bending vibrational modes. The upper dashed curve (stretch,  $b_o = b_i$ ) is for degenerate bend modes, while the lower solid curve (stretch,  $b_o \neq b_i$ , tunnel) includes the contribution from the first excited X-H stretch state (tunnel splitting) for non-degenerate bend modes.

these curves, which decreases (for the most part) with decreasing  $R$ . From Eq. (3), this leads to a drop in  $\Phi$ . The black curve in Figure 2 shows the fractionation ratio with only the O-H/D stretch zero-points included.

A countervailing influence on  $\Phi(R)$  comes from the bends, which harden in frequency with decreasing  $R$ . Figure 1 shows the zero-points only for the out-of-plane bends for the H and D cases. Their limiting values at large  $R$  are  $\frac{1}{2}\omega_{H,\perp,o}$  ( $=325 \text{ cm}^{-1}$ ) and  $\frac{1}{2\sqrt{2}}\omega_{H,\perp,o}$  ( $=230 \text{ cm}^{-1}$ ), respectively, where  $\omega_{H,\perp,o} = 650 \text{ cm}^{-1}$ . The corresponding trends for the in-plane bend (not plotted) are obtained from Eq. (5), setting  $\omega_{H,\perp,i} = 1600 \text{ cm}^{-1}$ . The consequences of the opposite trends for the hydrogen and deuterium bend and stretch frequencies — more compactly, competing quantum effects — has been the subject of much recent study [14, 26–30].

Presently, for  $\Phi$ , it is  $Z_H - Z_D$  that matters, which evidently also showcases the competition between the X-H bends and the X-H stretch. The solid blue curve in Figure 2 shows that the hardening of the bend modes with decreasing  $R$  significantly increases the fractionation ratio compared to the contribution from just the stretch mode. This is one of the main results of this paper. Kreevoy and Liang [13] previously pointed out that bending modes could alter their results for the correlation of  $\Phi$  and  $R$ . They gave the rough estimate that  $\Phi$  could be increased by a factor of about 1.7. Edison, Weinhold, and Markley also mentioned the effect of the bend modes [31],

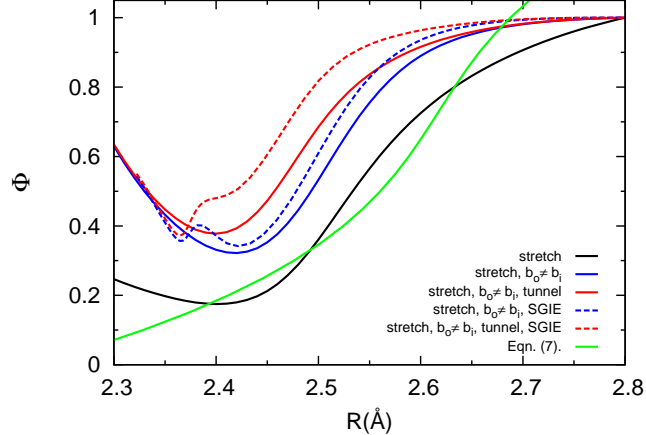


Figure 3. Corrections due to the secondary geometric isotope effect (SGIE) are shown as the dashed curves: the blue dashed line (stretch,  $b_o \neq b_i$ , SGIE) is without including tunneling and the red dashed line (stretch,  $b_o \neq b_i$ , tunnel, SGIE) is with tunneling. The solid curves of the same colour are from Figure 2, which do not include the SGIE. The green curve is the empirical function, defined by Eqn. (7), and given in Ref. 16. Note that the slight undulation in the dashed curves below 2.4 Å can be traced to the very rapid change of the SGIE ( $R_D - R_H$ ) in that region; see the lower panel of Figure 7 in Ref. 14.

finding values of  $\Phi > 1$  for weak bonds.

### B. Role of non-degeneracy of the bend modes

For the main results of this paper, the bend modes are made non-degenerate using Eq. (5) since the out-of-plane and in-plane modes are different in frequency in reality. We briefly investigate how different the fractionation factor would be if the degeneracy were retained.

The dotted blue curve in Figure 2 shows the plot of  $\Phi$  with both bends having frequencies corresponding to the out-of-plane mode. Evidently, the change is relatively small, but not negligible. As per the model, the smaller the bend frequency, the faster it hardens;  $\Omega_{\perp}(R)/\omega_{\perp} = \sqrt{1 + 2f(R)/\omega_{\perp}^2}$ . Hence, changing one of the bends frequencies to  $1600 \text{ cm}^{-1}$  reduces  $Z_H - Z_D$  relative to the degenerate case. Bend non-degeneracy can reduce the fractionation by about 10-20% compared to the degenerate case.



### C. Role of the tunnel splitting

For long H-bonds, the proton transfer potential has a high barrier and the tunnel splitting of the vibrational ground state is negligible [14]. However, for  $R < 2.55 \text{ \AA}$ , the splitting becomes significant, as can be seen in Figure 1. A multiplicative correction  $\Phi_{tun}$  (Eq. (6)) introduces the effect of the thermal population of the first low-lying excited state. This factor is always larger than one because the H tunneling splitting is larger;  $\delta E_H > \delta E_D$ . When the tunnel splitting is much larger than the thermal energy  $k_B T$  (i.e. for  $R < 2.4 \text{ \AA}$ ) the correction factor is extremely close to unity. When the tunnel splitting is much less than  $k_B T$  the correction factor is approximately  $(1 + (\delta E_H - \delta E_D)/2k_B T)$ .

Figure 2 shows that the tunnel splitting has a small but non-negligible effect in the range,  $R \sim 2.4 - 2.6 \text{ \AA}$ . We should also clarify the nomenclature here. For sufficiently small  $R$ , the barrier is no longer present, and so there is strictly no ‘‘tunnel splitting.’’ We just have two well-separated vibrational energies instead. Note that in a solvent there will be local dynamical fluctuations of the local electric field that couple to the electric dipole moment associated with the X-H stretch and for large enough fluctuations the tunnel splitting will not appear because it will be destroyed by quantum decoherence [32]. Also, when the proton affinity of the donor and acceptor differ by more than about  $500 \text{ cm}^{-1}$  (1.5 kcal/mol or 1.3 pK<sub>a</sub> units) this effect may be absent.

### D. Role of the secondary geometric isotope effect

The SGIE has a significant effect on the stretch mode vibrational frequencies for  $R \sim 2.4 - 2.5 \text{ \AA}$ , where the proton transfer barrier has effectively disappeared. Its inclusion yielded better agreement of the H/D stretch frequency ratio; compare Figure 8 in Ref. 14, where this ratio is 1 (1.15) with (without) SGIE, which is a sizeable change for strong short H-bonds.

Figure 3, however, points to a more modest influence of the SGIE on the fractionation ratio. The only significant effect is how it modifies the contribution from the tunnel splitting. Without the SGIE, the correction factor is approximately  $(1 + (\delta E_H(R) - \delta E_D(R))/2k_B T)$ . With the SGIE, the correction factor is approximately  $(1 + (\delta E_H(R_H) - \delta E_D(R_D))/2k_B T)$ . This is larger because  $R_D > R_H$ , and an increase in donor-acceptor distance of as little as  $0.02 \text{ \AA}$  for D relative to H can increase the energy barrier and thereby noticeably decrease  $\delta E_D(R_D)$  [14].

If tunneling contributions are suppressed by, e.g., a sizeable difference in pK<sub>a</sub>'s between the

donor and acceptor, the above analysis suggests that the SGIE would have only a small influence on the fractionation factor. The key effect that appears to govern the magnitude range of  $\Phi(R)$  according to our model is the competing quantum effect between the X-H stretch and X-H bends.

### E. Sensitivity to choice of reference distance

Calculation of  $\Phi$ , in Eqn. (2) requires knowledge of the ratio of H/D concentration in the solvent. In the reported calculations we took this ratio to be given by the value calculated within our model at  $R = 2.8 \text{ \AA}$ , approximately the relevant length in water. Our results are not particularly sensitive to this exact choice of this reference distance. For  $R > 2.7 \text{ \AA}$  the difference between the H and D zero-point energies is small. This can be seen from Figure 2. Even for the case of purely stretch modes taking the reference distance to be  $R = 2.7 \text{ \AA}$  would only increase  $\Phi(R)$  by about 10 per cent compared to the values shown in our curves.

### F. Comparison with experiment

To put our results in context we now briefly review previous measurements of  $\Phi$  that have been used to deduce a value for  $R$  in a specific molecule.

Based on calculations from an empirical one-dimensional quartic potential [23], Mildvan et al.[16] considered a relation between the fractionation factor and donor-acceptor distance,

$$R = (2.222 + 1.192\Phi - 1.335\Phi^2 + 0.608\Phi^3) \text{ \AA}. \quad (7)$$

It was used together with measurements of fractionation ratios for 18 H-bonds in several different enzymes to deduce the length  $R$ . The values they obtained for  $R$  were mostly in agreement with values of  $R$  deduced from NMR chemical shifts, and from X-ray crystallography. Values of  $\Phi$  ranged from 0.32 to 0.97 and the corresponding values of  $R$  were in the range 2.49 to 2.68  $\text{\AA}$ . However, Figure 3 shows significant differences between equation (7) and our results.

Klug et al.[33] studied crystals of the dihydrated sodium salt of hydrogen bis(4-nitrophenoxide) and found a fractionation ratio of  $0.63 \pm 0.04$ . Using the Kreevoy and Liang [13] parametrisation, they noted that this value was inconsistent with the bond length observed via X-rays,  $R = 2.452 \text{ \AA}$ , and with the value of  $\Phi = 0.31 \pm 0.03$  deduced from UV spectroscopy for bis(4-nitrophenoxide) in acetonitrile solution. Consequently, they suggested that “the solid was not in isotopic equilibrium

with the solvent from which it was precipitated.” However, their results are consistent with our parameterisation of  $\Phi$  versus  $R$ , if tunnel splitting is not included.

Loh and Markley[34] found fractionation factors in the range 0.28-1.47 for the different H-bonds in the protein staphylococcal nuclease. Clearly, we cannot explain their  $\Phi$  values larger than unity. However, it should be pointed out that many of these bonds are weak with donor-acceptor distances in the range,  $R \sim 2.8 - 3.3 \text{ \AA}$  and that no clear correlation was observed between the values of  $\Phi$  and  $R$ . Loh and Markley did note a difference between the fractionation factors of backbone amide bonds that are solvent-exposed (average value 0.98) and those that are not (average value 0.79). This observation is consistent with what one might anticipate: solvent accessibility could affect the effective  $\text{pK}_a$  of the donor and/or acceptor. A consequent change (increase) in distance between them may also ensue. These would lead to a weakening of the H-bond, and therefore move  $\Phi$  values closer to 1. In the model we employ, this solvent effect would enter parametrically as a difference in effective  $\text{pK}_a$  and donor-acceptor distance. However, the works of Khare *et al.* [35] and LiWang and Bax [36] point to minimal effects. The former, which reported on the immunoglobulin G binding domains of protein G, found little difference between average fractionation factors (average  $\Phi$  of 1.05 for  $\alpha$ -helical, 1.13 for  $\beta$ -sheet, and 1.08 for solvent-exposed residues). LiWang and Bax gave similar findings for ubiquitin. A recent study of the core of protein Kinase A also found no correlation between  $\Phi$  values and secondary structure [37].

Thakur *et al.*[38] have recently developed a new method for the rapid determination of H/D exchange from two-dimensional NMR spectra. Section S5 of their Supplementary material shows fractionation values for three different proteins. For 80 different amino acid residues in Tim23, the values ranged from 0.81 to 1.73. For 58 different amino acid residues in Ubiquitin, the values ranged from 0.34 to 1.67. For 54 different amino acid residues in Dph4, the values ranged from 0.45 to 2.04.

Recently, an extensive study was made of mutants of the Green Fluorescent Protein with a short H-bond between the chromophore and the amino acid Asp148 [21]. The donor-acceptor bond length estimated from X-ray structures was  $2.4 \pm 0.2 \text{ \AA}$ . The  $\text{pK}_a$  of the chromophore was systematically varied by 3.5 units through halogen substitutions. This range covers the  $\text{pK}_a$  matching (degenerate diabatic states) required for strongest bonds [17]. The experimental results were compared to calculations based on a one-dimensional proton transfer potential based on same diabatic state model used here. The measured fractionation factors (deduced from analysis of UV

absorption spectra) were in the range 0.54 - 0.9, taking a minimum value for  $pK_a$  matching. This observation and a value of  $\Phi = 0.54$  for  $R = 2.4 \pm 0.2 \text{ \AA}$  are consistent with our analysis when the bend modes and tunnel splitting are taken into account.

Edison, Weinhold, and Markley performed *ab initio* calculations for a wide range of peptide clusters [31]. They observed a correlation between the fractionation ratio and the donor-acceptor distance. For  $R > 2.55 \text{ \AA}$ , the fractionation was larger than one, and for  $R \simeq 2.45 \text{ \AA}$ ,  $\Phi \simeq 0.6$ .

#### IV. CONCLUSIONS

We have shown that the H/D fractionation factor  $\Phi$  is quite sensitive to the donor-acceptor distance  $R$  in hydrogen bonds, and so, in principle, can be used as a “ruler” for determining bond lengths. However, caution is in order because there are a number of subtle effects that modify the exact form of the relationship between  $\Phi$  and  $R$ . These include competing quantum effects between stretch and bend modes, non-degeneracy of the bend modes, tunnel splitting, the secondary geometric isotope effect, and differences between the proton affinity of the donor and acceptor.

Our results raise questions about whether values of  $\Phi$  as small as 0.3 are really possible for short bonds, contrary to some measurements and previous theoretical claims. Equally, our results cannot explain  $\Phi$  values that are much larger than 1 for long bonds. The discrepancy for short bonds may be due to our assumption that the stretch and bend modes are independent. Although our model quantitatively describes many experimental results for bond lengths, vibrational frequencies, and isotope effects, for  $R \sim 2.45 \text{ \AA}$ , it does give stretch mode frequencies that are higher than observed. (See Figure 6 in Ref. 14 and the associated discussion.) This would also lead to a larger fractionation factor than observed. Addressing this issue will require a systematic investigation of solutions to the vibrational Schrodinger equation for a higher-dimensional (probably four dimensional) potential energy surface. We leave that for a future study.

#### ACKNOWLEDGMENTS

We thank Michael Ashfold, Steve Boxer, Stephen Fried, Tom Markland, Seth Olsen, Luke Oltrogge, and Lu Wang for helpful discussions. RHM received financial support from an Aus-

tralian Research Council Discovery Project grant.

---

- [1] W. Cleland and M. Kreevoy, *Science* **264**, 1887 (1994).
- [2] C. N. Schutz and A. Warshel, *Proteins: Structure, Function, and Bioinformatics* **55**, 711 (2004).
- [3] A. Das, V. Prashar, S. Mahale, L. Serre, J. L. Ferrer, and M. V. Hosur, *Proceedings of the National Academy of Sciences* **103**, 18464 (2006).
- [4] W. W. Cleland, *Advances in Physical Organic Chemistry* **44**, 1 (2010).
- [5] C. Perrin, *Accounts of Chemical Research* **43**, 1550 (2010).
- [6] M. Hosur, R. Chitra, S. Hegde, R. Choudhury, A. Das, and R. Hosur, *Crystallography Reviews* **19**, 3 (2013).
- [7] M. Nadal-Ferret, R. Gelabert, M. Moreno, and J. M. Lluch, *Journal of the American Chemical Society* **136**, 3542 (2014).
- [8] J. D. Graham, A. M. Buytendyk, D. Wang, K. H. Bowen, and K. D. Collins, *Biochemistry* **53**, 344 (2014).
- [9] J. P. Klinman, *ACS Central Science* **1**, 115 (2015).
- [10] D. A. Nichols, J. C. Hargis, R. Sanishvili, P. Jaishankar, K. Defrees, E. W. Smith, K. K. Wang, F. Prati, A. R. Renslo, H. L. Woodcock, and Y. Chen, *Journal of the American Chemical Society* **137**, 8086 (2015).
- [11] T. Harris, Q. Zhao, and A. Mildvan, *Journal of Molecular Structure* **552**, 97 (2000).
- [12] One might also consider whether the fact that X-ray crystal structures are refined with classical molecular dynamics using force fields that are parametrised for weak H-bonds may also be a problem. Such refinements may naturally bias towards weak bonds, i.e., the longer bond lengths that are common in proteins.
- [13] M. Kreevoy and T. Liang, *Journal of the American Chemical Society* **102**, 3315 (1980).
- [14] R. H. McKenzie, C. Bekker, B. Athokpam, and S. G. Ramesh, *The Journal of Chemical Physics* **140**, 174508 (2014).
- [15] F. Hibbert and J. Emsley, *Advances in Physical Organic Chemistry* **26**, 255 (1990).
- [16] A. S. Mildvan, M. A. Massiah, T. K. Harris, G. T. Marks, D. H. T. Harrison, C. Viragh, P. M. Reddy, and I. M. Kovach, *Journal of Molecular Structure* **615**, 163 (2002).
- [17] R. H. McKenzie, *Chemical Physics Letters* **535**, 196 (2012).

- [18] G. Gilli and P. Gilli, *The Nature of the Hydrogen Bond* (Oxford U.P., Oxford, 2009).
- [19] L. Wang, S. D. Fried, S. G. Boxer, and T. E. Markland, *Proceedings of the National Academy of Sciences* **111**, 18454 (2014).
- [20] Y. Kanematsu and M. Tachikawa, *The Journal of Chemical Physics* **141**, 185101 (2014).
- [21] L. M. Oltrogge and S. G. Boxer, *ACS Central Science* **1**, 148 (2015).
- [22] R. H. McKenzie, *The Journal of Chemical Physics* **141**, 104314 (2014).
- [23] D. Bao, W. P. Huskey, C. A. Kettner, and F. Jordan, *Journal of the American Chemical Society* **121**, 4684 (1999).
- [24] D. T. Colbert and W. H. Miller, *The Journal of Chemical Physics* **96**, 1982 (1992).
- [25] M. Ichikawa, *Journal of Molecular Structure* **552**, 63 (2000).
- [26] X.-Z. Li, B. Walker, and A. Michaelides, *Proceedings of the National Academy of Sciences* **108**, 6369 (2011).
- [27] S. Habershon, T. E. Markland, and D. E. Manolopoulos, *The Journal of Chemical Physics* **131**, 024501 (2009).
- [28] T. Markland and B. Berne, *Proceedings of the National Academy of Sciences* **109**, 7988 (2012).
- [29] G. Romanelli, M. Ceriotti, D. E. Manolopoulos, C. Pantalei, R. Senesi, and C. Andreani, *The Journal of Physical Chemistry Letters* **4**, 3251 (2013).
- [30] L. Wang, M. Ceriotti, and T. E. Markland, *The Journal of Chemical Physics* **141**, 104502 (2014).
- [31] A. S. Edison, F. Weinhold, and J. L. Markley, *Journal of the American Chemical Society* **117**, 9619 (1995).
- [32] J. P. Bothma, J. B. Gilmore, and R. H. McKenzie, *New Journal of Physics* **12**, 055002 (2010).
- [33] C. A. Klug, P. L. Lee, I. S. H. Lee, M. M. Kreevoy, R. Yaris, and J. Schaefer, *The Journal of Physical Chemistry B* **101**, 8086 (1997).
- [34] S. N. Loh and J. L. Markley, *Biochemistry* **33**, 1029 (1994).
- [35] D. Khare, P. Alexander, and J. Orban, *Biochemistry* **38**, 3918 (1999).
- [36] A. C. LiWang and A. Bax, *Journal of the American Chemical Society* **118**, 12864 (1996).
- [37] G. C. Li, A. K. Srivastava, J. Kim, S. S. Taylor, and G. Veglia, *Biochemistry* **54**, 4042 (2015).
- [38] A. Thakur, K. Chandra, A. Dubey, P. D'Silva, and H. S. Atreya, *Angewandte Chemie International Edition* **52**, 2440 (2013).